Visual Abstract

Prediction of mechanical behavior of epoxy polymer using Artificial Neural Networks (ANN) and Response Surface Methodology (RSM)

Khalissa Saada, Salah Amroune, Moussa Zaoui
Department of Mechanical Engineering, University of Mohamed Boudiaf-M'Sila, Algeria. Laboratoire de Matériaux, et Mécanique des Structures (LMMS), Université de M'sila. Algérie.
Khalissa.saada@univ-msila.dz, https://orcid.org/0000-0002-3025-1287
salah.amroune@univ-msila.dz, https://orcid.org/0000-0002-9565-1935
moussa.zaoui@univ-msila.dz, https://orcid.org/0009-0005-7178-2542

ABSTRACT. The aim of this study is to analyze the effect of different geometries and sections on the mechanical properties of epoxy specimens. Five tensile tests were carried out on three types of series. The experimental results obtained were 1812.21 MPa, 3.90% and 41.91 MPa for intact specimens, 1450.41 MPa, 2.16% and 21.28 MPa for specimens with hole and 750.77 MPa, 2.77% and 11.89 MPa for specimens with elliptical -notched for Young's Modulus , strain and stress respectively. In addition, the experimental results indicated that the mechanical properties of both (Young's Modulus value and stress value) were higher in an intact specimen. Afterwards, the nonlinear functional relationship of input parameters between epoxy sample geometries and sections was established using the response surface model (RSM) and the artificial neural network (ANN) to predict the output parameters of mechanical properties (Young's Modulus and stress). In addition, the design of experiment was developed by the Analysis of the Application of Variance (ANOVA). The results showed the superiority of the ANN model over the RSM model, where the correlation coefficient values for the model datasets exceed ANN (R^2 = 0.984 for Young's Modulus and R^2 = 0.981 for the stress).

KEYWORDS. ANN, Mechanical properties, ANOVA, RSM, Epoxy, Geometry.

OPEN ACCESS

Citation: Saada, K., Amroune, S., Zaoui, M., Prediction of mechanical behavior of epoxy polymer using Artificial Neural Networks (ANN) and Response Surface Methodology (RSM), Frattura ed Integrità Strutturale, 66 (2023) 191-206.

Received: 28.05.2023
Accepted: 11.08.2023
Online first: 16.08.2023
Published: 01.10.2023

INTRODUCTION

Thermosetting polymers are widely used in various scientific aspects and engineering applications such as wind, aerospace, astronautics, automotive and military industries. There are several types of polymers, for example polyester [1, 2], styrene [3, 4], acrylic [5, 6] and epoxy [7, 8]. Epoxy resin is one of the most important polymers

because of its advantages, such as hardness, corrosion resistance and relatively low cost [9-12]. It is preferred because of its mechanical properties [13] including tensile and bending.[14, 15] explained that sample dimensions and geometry affect mechanical properties.[16, 17] They found that there is a gradual decrease in mechanical properties as the diameter of the hole increases in the geometry of the samples. According to habibi et al .[18] They fabricated samples of 6mm open hole bio-flax flakes with different stacking sequences [0]12, $[0\ 90]_{6s}$ and $[0\ +45\ 90\ -45]_{3s}$. The results of the tensile tests showed the effect of the 6 mm open hole on the performance of the laminate. For that, dimensions are of great importance for mechanical performance, as indicated by han et al [19] They found that increasing geometric dimensions increases the stress of manufactured bee samples.

Recently, to predict the mechanical properties of samples of materials such as aluminum, composites and polylactic acid PLA, researchers have used models like ANN and RSM [20-23]. It is possible to use an artificial neural network (ANN) which is one of the most applicable means of nonlinear analysis to determine the relationships between input and output, and to allow the prediction of the output parameter with ANN[24]. Response surface methodology (RSM) uses distinct combinations of experimental design to determine linear, quadratic, and interaction terms that provide optimal performance from a given set of response factors and variables [25]. Boumaaza et al. [26] applied the two techniques together, RSM and ANN, to predict the results of the bending test of compounds for bending strength, displacement and flexural modulus, and found that the ANN model had higher accuracy than the RSM model. While, Choudhary et al [27] predicted the corrosion behaviour of tensile and bending samples consisting of fiber-reinforced epoxy compounds using both ANN and RSM methods. But, Alhijazi et al .[28] used the artificial neural network (ANN) model to predict the mechanical properties of composite samples of epoxy with palm fibre and luffa fibres, where the results showed that the percentage of fibres had a higher effect on the tensile test results.

Therefore, the objective of this paper is to use the methodology of neural networks (ANN) and response surfaces (RSM) to predict the mechanical properties of epoxy samples (undamaged specimen, specimen with hole-notched and specimen with elliptical -notched). To evaluate the effect of input parameters such as sample geometry and sample cross-section, the expected results of ANN and RSM, it were analyzed and compared with experimental results after sample preparation, tensile testing, and analysis of experimental results, with important conclusions.

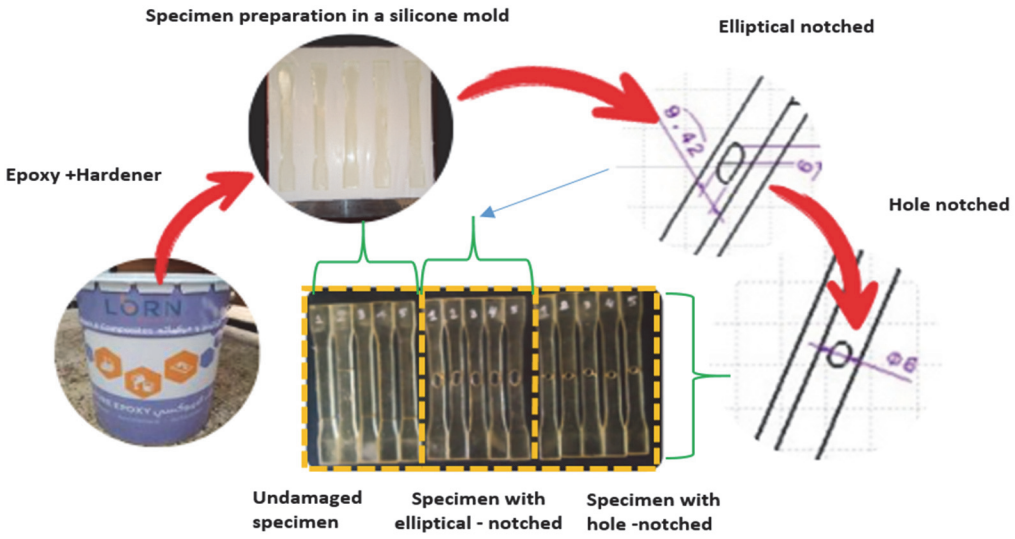

Figure 1: Epoxy sample preparation steps.

MATERIALS AND METHODS

Sample preparation and quality control

The specimen were produced using the epoxy where LORN Chemicals' epoxy was used by an Algerian company located in the Bouira region , The chemical formula of epoxy is C3H13N3, and it is a type of polymer with wide applications that is attracting the interest of many researchers because of its properties[26, 29, 30] . In our study, three different epoxy engineering models (undamaged specimen, specimen with hole-notched and specimen with elliptical- notched) were used according to ASTM D638-14 with uniform dimensions of 165 x 12 mm2 and a thickness of 7 mm, and each model has five samples. In this work, the resin was mixed with hardener at the rate of 65% by weight and

35% by weight, and then placed in a silicone mold that was manufactured previously. The samples were left in the mould to dry for 24 hours and then heat-treated at 70°C for 5 hours. The total samples obtained were 15 samples. After heat treatment, five samples were left as is, five samples were drilled with a diameter of 6 mm, and the last five were drilled with an oval hole measuring 6 x 3 mm. These dimensions have been addressed by many researchers, for example[32 ,31]. The method of moulding the sample is illustrated in Fig. 1.

ANN AND RSM METHOD

In Mechanical/Material Science, both Artificial Neural Networks (ANN) and Response Surface Methodology (RSM) find various applications. ANN excels in predicting material properties, optimizing manufacturing processes, and non-destructive testing, while RSM is valuable for experimental design, surface modification, and alloy design. When used together, they synergistically enhance problem-solving capabilities, leading to accurate predictions, efficient processes, and innovative material designs, advancing the field significantly. Both ANN and RSM were used in the study to predict the mechanical properties of epoxy specimens based on their geometries and sections. These models serve as tools to understand how variations in the epoxy sample's configuration affect its mechanical behavior. The comparison between ANN and RSM in this study revealed that the ANN model was superior in predicting the mechanical properties compared to the RSM model. This suggests that the relationships between the input parameters (geometries and sections) and output properties (Young's Modulus and stress) are complex and non-linear. ANN's ability to capture and learn non-linear patterns made it more suitable for this particular problem.

Artificial Neural Network (ANN) Method

It is an algorithm for calculating nonlinear maps that consists of an artificial neural network simulating the functioning of the biological nervous system, inspired by nature [33-35]. Fig. 2 shows the computational unit of this artificial neural network, consisting of one or two hidden layers, as well as input layers where each input x_i is represented by a single neuron, and an output layer y_i that synthesizes the information processed from the input, w are the weight values where k are the biases, as shown in Eqn. 1[36].

$$y_i = \frac{1}{1+e^{kx_i}} \tag{1}$$

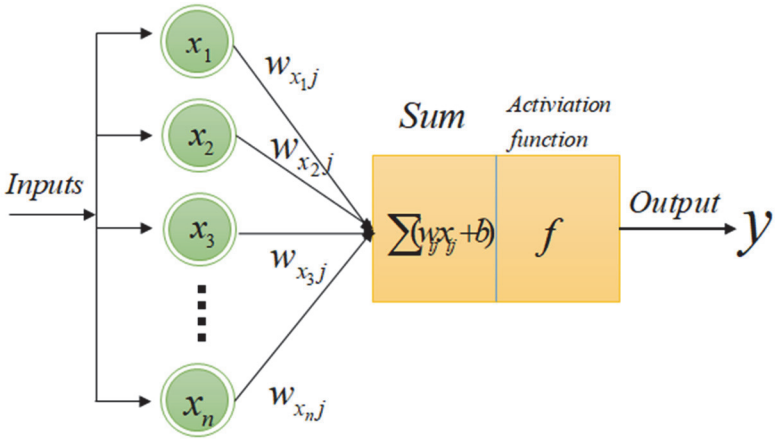

Figure 2: Artificial neuron.

Response Surface Methodology (RSM) Method

Response surface methodology is a technique for modeling, analyzing, and simulating problems with multiple response variables and multiple independent variables. It involves the use of mathematical, statistical and graphical methods to develop mathematical models that optimize the experimental process. In addition, these models make it possible to establish correlations between the input and response variables obtained during the experiments [37, 38].

In Tab. 1, the associated parameters are presented as well as their names and to model them in order to obtain the outputs represented in the mechanical wicker of the tensile test, the linear and quadratic method (surface response methodology) was used and they are defined according to the following relationship [39]:

$$Y(x) = B_0 + \sum_{j=1}^{k} B_j X_j + \sum_{j=1}^{k} B_{jj} X_j^2 + \sum_{j=1}^{k} \sum_{i \geq 2}^{k} B_{ji} X_j X_i \quad (2)$$

where Y(x) represents the bound predicted response. In addition, Xi and Xj correspond to the independent variables, while B_0, B_j, B_{jj} and B_{ji} denote a constant, linear first-order interaction and second-order interaction coefficients, respectively.

Symbol	Factor	Unit	Levels		
			Low level (1)	Intermediate level (0)	High level (+1)
A	Geometry	-	-1	0	1
B	Section	mm^2	83.91	92.50	102.00

Table 1: RSM factors levels.

CHARACTERIZATION TESTS OF EPOXY SAMPLES

After preparing epoxy samples (undamaged specimen, specimen with hole-notched and specimen with elliptical - notched) conforming to ASTM D638-14 and having dimensions of 165×19×7 mm^3, the tensile test was carried out using a tensile machine at the laboratory of the University of Boumerdes in Algeria. For this, both ends of the samples were attached to a length of 25 mm each on a traction clamp that helped to increase grip and prevent slippage, while the rate of control of the transmission speed was 1 mm/min. The samples were stretched to failure, as shown in Fig. 3, to obtain tensile results, such as the stress-strain curve and the Young's Modulus.

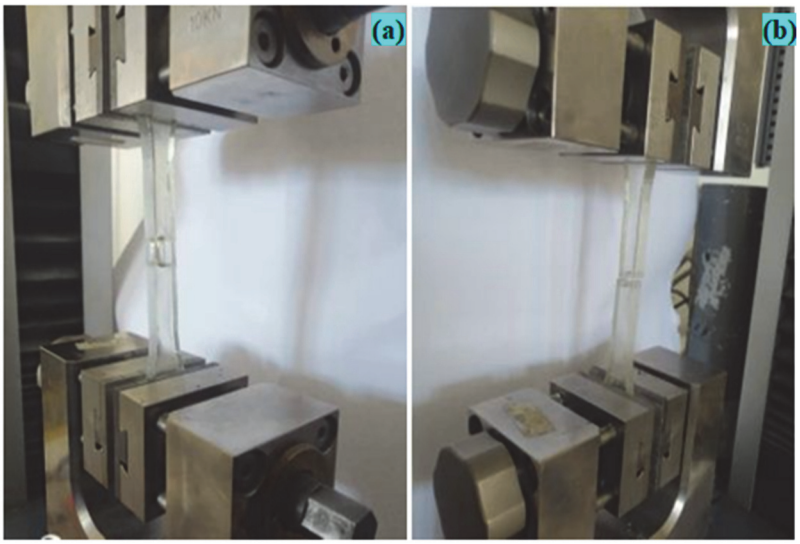

Figure 3: Tensile test (a) Specimen with elliptical- notched (b) Specimen with hole-notched.

RESULT AND DISCUSSION

Experimental results

Fig. 4 shows the standard deviation results for the three epoxy samples, namely the intact specimen, the hole-notched specimen and the elliptical- notched specimen, for each of the Young modules, stresses and strains. It can be observed that the diameter and shape of the hole have an effect on the mechanical properties, as shown in Fig. 4-a which shows the average Young's Modulus for five tensile tests on the three epoxy samples. The average Young's Modulus was higher than that of the undamaged specimen with a value of 1812.2±61.05, while it was lower for the

specimen with hole (1450.41±162.51) and the specimen with elliptical -notched (750.77±198.53). While Fig. 4-b shows the mean stress values for the three epoxy samples. Since the stress is also affected by the geometry of the samples, it is observed that the larger the diameter of the hole, the lower the stress. The mean stress values indicate 41±2.45, 21±2.17 and 11.89±4.3 for each specimen: undamaged, with hole and with elliptical- notched. On the other hand, the Fig. 4-c presents the results of the parametric deviation of the deformation. We observe that the undamaged specimen had a mean deformation value of 3.90±0.47, while the mean deformation value of the specimen with hole-nothed was 2.16±0.13. The mean deformation value of the specimen with elliptical- notched was 2.77±0.64. Similar results have already been reported on the effect of hole diameter on mechanical properties.[40, 41]

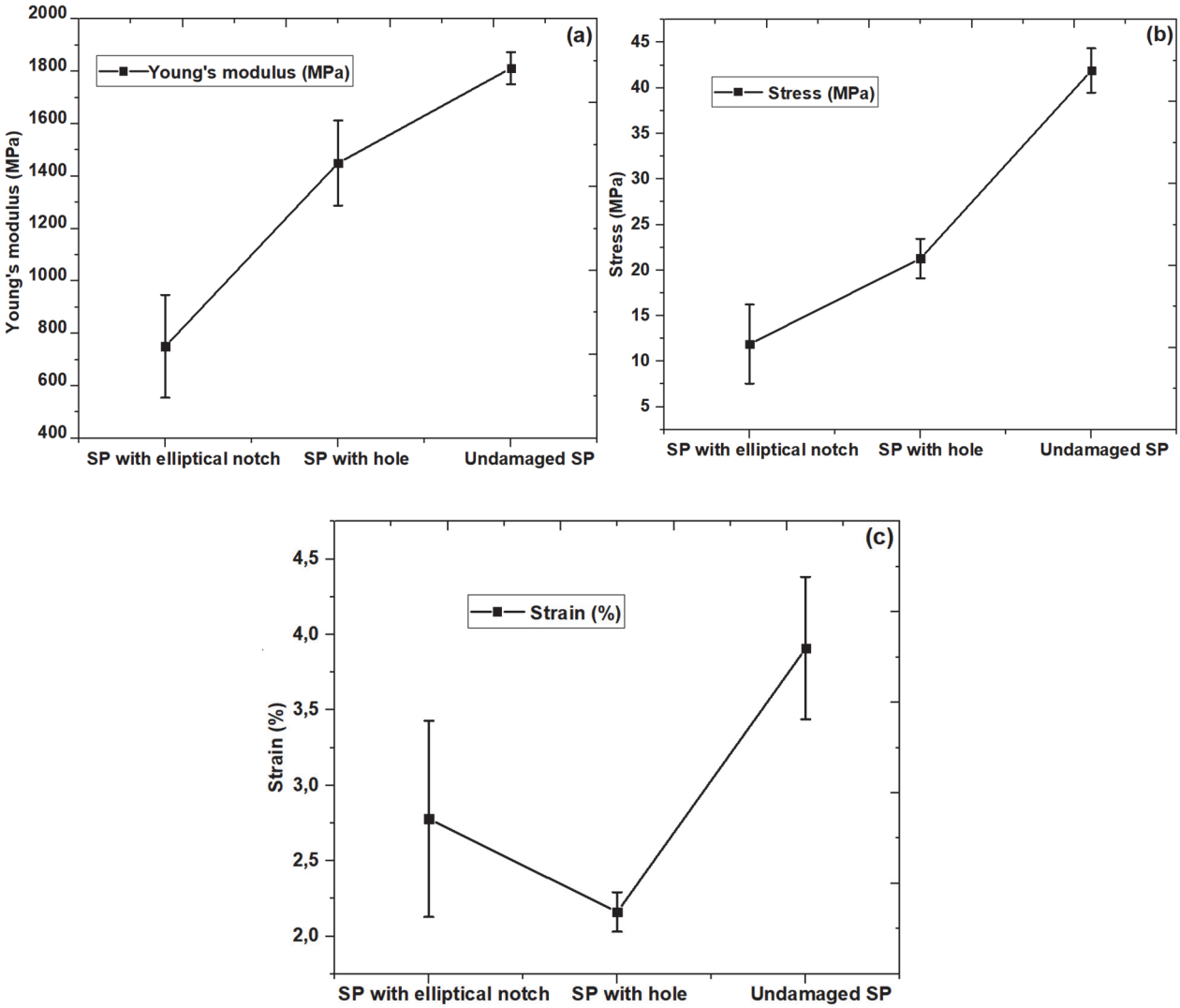

Figure 4: Mechanical test results: (a) Young‘s Modulus, (b) stress and (c) strain.

In Fig. 5, experimental results for: undamaged specimen, specimen with hole-notched and specimen with elliptical -notched, we can see a curve representing the mean values for the three samples (undamaged specimen, specimen with hole -notched and specimen with elliptical- notched) of stress-strain. The results showed the effect of sample geometry on mechanical properties during tensile tests. For example, the maximum stress value was recorded for the intact specimen with a value of 41.95 MPa and a strain of 4.05%, while the maximum stress value for the hole specimen was 21.06 MPa and a strain value of 2.10%. The maximum stress for the specimen with elliptical-notched was 14.17 MPa and the deformation was 2.89%. The results show that the length of the aperture has an influence on the results of the tensile tests of the samples and on the stress, which is consistent with previous research [36,42].

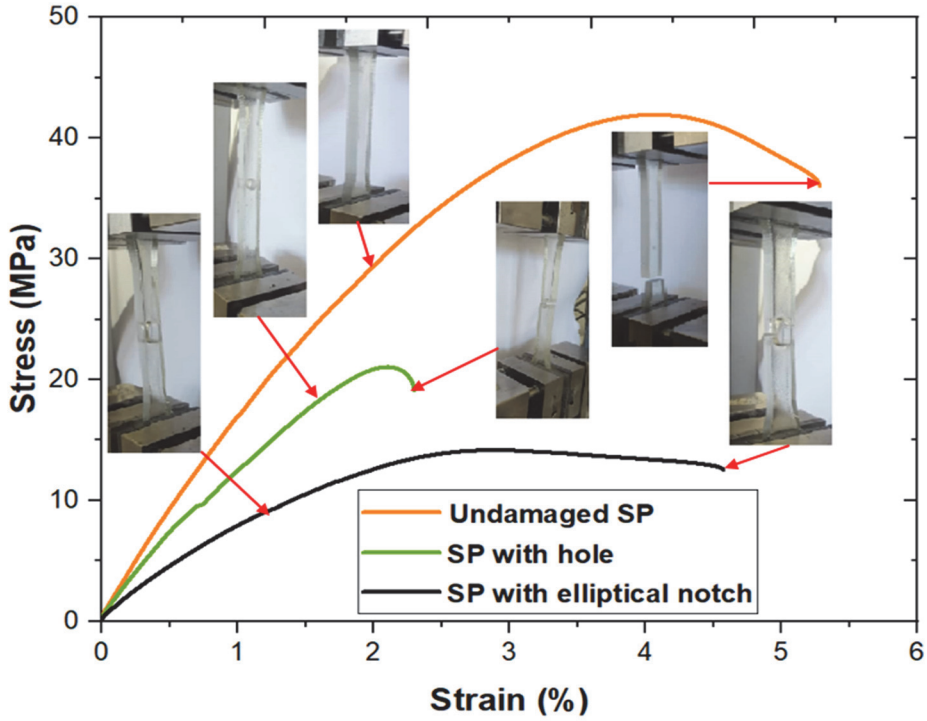

Figure 5: Experimental results for: undamaged specimen, specimen with hole-notched and specimen with elliptical –notched.

RSM modelling

In Tab. 2, experimental results are listed with models (ANN and RSM) according to two inputs, reflecting sample geometry and sample cross-sections, with either Young's Modulus or stress as output.

N°	Input variables		Output variables					
	Geometry	Specimen section (mm^2)	Maximum Stress (MPa)			Young's Modulus (MPa)		
			EXP	ANN	RSM	EXP	ANN	RSM
1	-1	102.555	18.404	19.204	19.518	1261.79	1375.474	1311-084
2	-1	97.524	21.060	21.051	20.793	1423.36	1448.134	1410-441
3	-1	83.913	24.221	24.180	24.078	1684.47	1719.382	1671-552
4	-1	102.684	20.391	19.602	19.485	1356.42	1364.197	1308-516
5	-1	90.2979	22.366	22.672	22.567	1526.02	1465.360	1550-464
6	0	88.33	11.008	9.425	12.078	545.09	617.176	760-212
7	0	86.7162	5.6846	10.957	11.79	967.12	953.758	745-283
8	0	84.6945	11.213	12.134	11.425	547.59	617.706	726-357
9	0	86.296	17.404	11.507	11.715	899.84	887.028	741-370
10	0	90.5692	14.171	14.047	12.471	794.25	555.458	780-666
11	1	86.31	45.767	41.610	41.899	1858.00	1847.381	1812-549
12	1	85.4642	41.950	41.775	41.396	1836.78	1857.097	1824-658
13	1	87.4324	42.132	41.211	42.566	1713.70	1719.878	1796-414
14	1	87.318	40.133	41.255	42.498	1858.79	1748.445	1798-062
15	1	85.1332	39.576	41.794	41.198	1793.80	1857.939	1829-385

Table 2: Experimental and modeling results of stress and Young's Modulus.

Source	Sum of Squares	df	Mean Square	F-value	p-value	
(a) ANOVA for Stress						
Model	2375.66	5	475.13	42.93	< 0.0001	significant
A-geometry	82.39	1	82.39	7.44	0.0233	
B-section(mm²)	0.8368	1	0.8368	0.0756	0.7895	
AB	3.97	1	3.97	0.3588	0.5639	
A²	1114.95	1	1114.95	100.74	< 0.0001	significant
B²	0.0028	1	0.0028	0,0003	0.9876	
Residual	99.60	9	11.07			
Cor Total	2475.27	14				
R^2 =0.9598, R^2 adjusted = 0.9374, R^2 predicted = 0.9267and Adequate precision =14.8008						
(b) ANOVA for Young's Modulus						
Model	3-014E+06	5	6-028E+05	31-40	< 0.0001	significant
A-geometry	1-941E+05	1	1-941E+05	10-11	0-0112	
B-section(mm²)	1993-83	1	1993-83	0-1039	0-7546	
AB	10258-86	1	10258-86	0-5344	0-4834	
A²	1-016E+06	1	1-016E+06	52-91	< 0.0001	
B²	2-99	1	2-99	0-0002	0-9903	
Residual	1-728E+05	9	19196-36			
Cor Total	3-187E+06	14				
R^2 =0.9458, R^2 adjusted = 0.9157, R^2 predicted = 0.8678 and Adequate precision =12.4394						

Table 3: ANOVA of quadratic model obtained for stress and Young's Modulus.

To develop empirical models for mechanical properties and analyze the influence of selected parameters, an experimental plan was designed using the Response Surface Methodology (RSM) technique, ANOVA (Analysis of Variance) is a statistical method used to assess the significance of different factors in a regression model, including quadratic models. In the context of a quadratic model, ANOVA helps to determine whether the quadratic term makes a significant contribution to the overall fit of the model. A quadratic model is a type of regression model that includes both linear and quadratic terms The ANOVA table for a quadratic model breaks down the total variation in the data into different components, each corresponding to the variation explained by the model or its components. It helps to evaluate the significance of each term (linear and quadratic) in the model and how much of the variation they account for. The ANOVA table typically consists of several components:

- Sum of Squares (SS): This represents the sum of the squared differences between the observed values and the predicted values from the model.
- Degrees of Freedom (DF): The degrees of freedom for each component represent the number of independent pieces of information available for estimating that component.
- Mean Square (MS): The Mean Square is obtained by dividing the Sum of Squares by its corresponding Degrees of Freedom.
- F-ratio (F-value): The F-ratio is calculated by dividing the Mean Square for a given component by the Mean Square of the residual (error) term.
- P-value: The p-value represents the probability of obtaining an F-ratio as extreme as observed, assuming that the null hypothesis is true (i.e., the term does not contribute significantly to the model).

If the p-value associated with the quadratic term (β2) is small (usually less than a chosen significance level, often 0.05), it indicates that the quadratic term is statistically significant, and its inclusion in the model improves the fit significantly. On the other hand, if the p-value is large, it suggests that the quadratic term does not contribute significantly to the model, and a simpler linear model might be more appropriate. ANOVA of a quadratic model assesses the significance of the quadratic term (x^2) and helps determine if it improves the model's performance compared to a simpler linear model. RSM was used, which was used in the previous literature in the case of tensile tests and its results were good [43,44]. The

experimental results were then analyzed using Design-Expert 12 software. The findings and their implications are discussed in the subsequent section and subsections, corresponding to the output responses obtained from the analysis
To create mathematical equations between input and output variables of tensile epoxy samples, RSM was used. The data were made using the ANOVA variance shown in both Tabs. 3 and 4 for Young's coefficient and stress, where The effectiveness of a term is determined by the p-value, where the smaller the p-value, the better the expected results based on what we obtained< 0.0001[45]. The ANOVA results suggest that the first-order parameters A (sample geometry), B (section parameter), and AB (geometry parameter multiplied by section parameter), as well as the square sample geometry parameter A^2 and the square parameter of sampling section B^2, have a significant impact on the mechanical properties (Young's Modulus and stress). These parameters, along with the geometry parameter A^2 of sample 2, are the most important predictors of the mechanical properties. Overall, the regression models' values indicate a good fit, as they are greater than 80%. For the Young's Modulus, we can observe a correlation coefficient R^2 of 0.95 and an adjusted coefficient R^2 of 0.91. As for the stress, the correlation coefficient R^2 indicated 0.94, and the adjusted coefficient R^2 was 0.91. These are excellent results, consistent with previous research. In addition, the accuracy of the models for stress and Young's Modulus can be tested by graphs expressed by the Design Expert for each actual or forecast period, in Fig. 6(a-d). The normal probability with respect to the residuals in Fig. 6(b-e), the residuals with respect to the values predicted in Fig. 6(c-f),indicates that the expected values are in a straight line with the actual values and, therefore, there is no evidence that the results are uneven or abnormal. The equations for RSM models - generated using experimental data for sample geometric responses and sample sections were presented as follows:

$$\text{Young's Modulus} = 1777.49 - 355.7A - 52.228B + 132.93AB - 627.66A2 + 1.90B2 \quad (3)$$

$$\text{Stress} = 12.81 + 11.76A + 1.63B + 3.95AB + 20.99A20.0588B2 \quad (4)$$

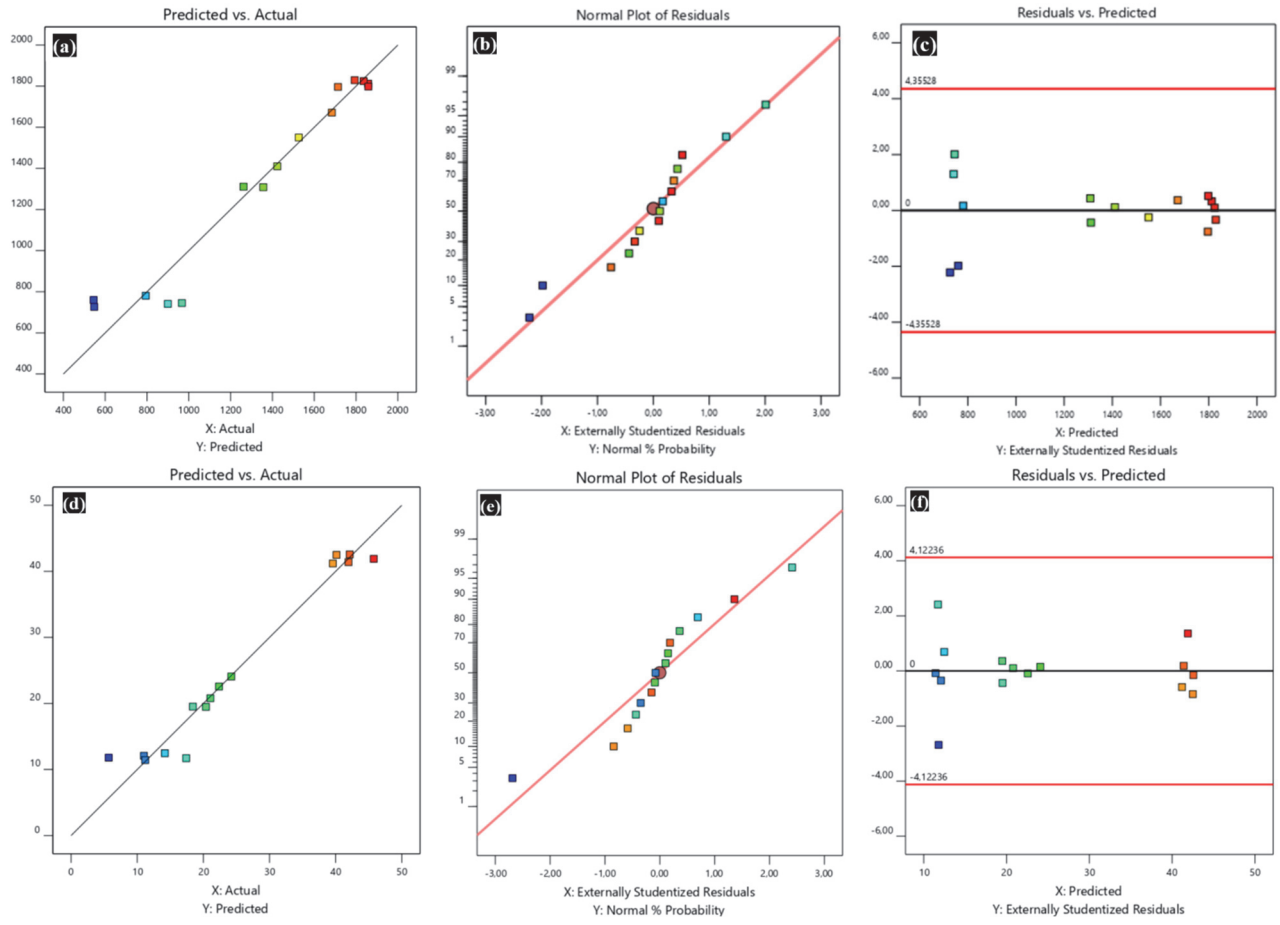

Figure 6: Plots of stress and Young's Modulus of epoxy samples conductivity model; (a)-(d) actual vs. predicted, (b)-(e) normal probability vs. residuals, and (c) -(f) residuals vs. predicted.

Fig. 7 shows three-dimensional surface diagrams resulting from the Design-expert design for each of Young's Modulus Fig. (7-a). Where the effect of the geometry of the specimens and sections of the specimens on the value of the Young's Modulus can be observed. The red area indicates the highest value that the Young's Modulus can take, which can reach 1858.79 MPa, and the blue area at the lowest value approximately at 545.09 MPa. Fig. (7-b) indicates that the stress value is the other, where the highest value is higher when the Specimen is intact where the red area indicates the highest stress, which can reach 45.76MPa and the lowest stress in the blue area at 5.68MPa. Fig. 8 shows the numerical ramps for the optimum stress and Young's Modulus where the maximum desirability was 0.95 with a sample section area of 86.36 mm² and the geometry of the samples at -0.1 and these optimal values for the tensile test for Young's Modulus and the stresses should be 45.76MPa and Young's Modulus of 1858.79MPa.

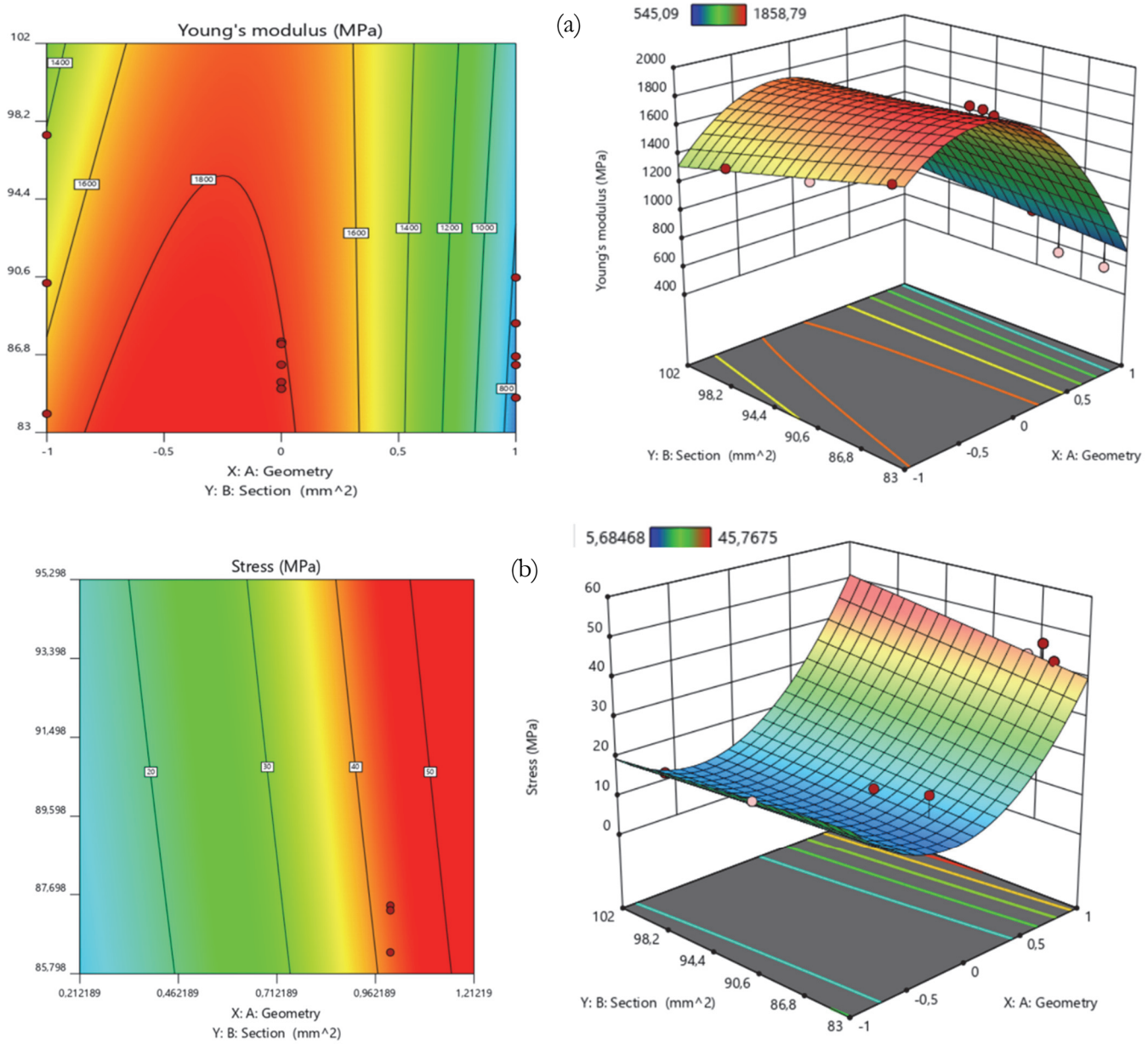

Figure 7: Contour trace with their 3D response surface plot for (a) Young's Modulus, (b) stress.

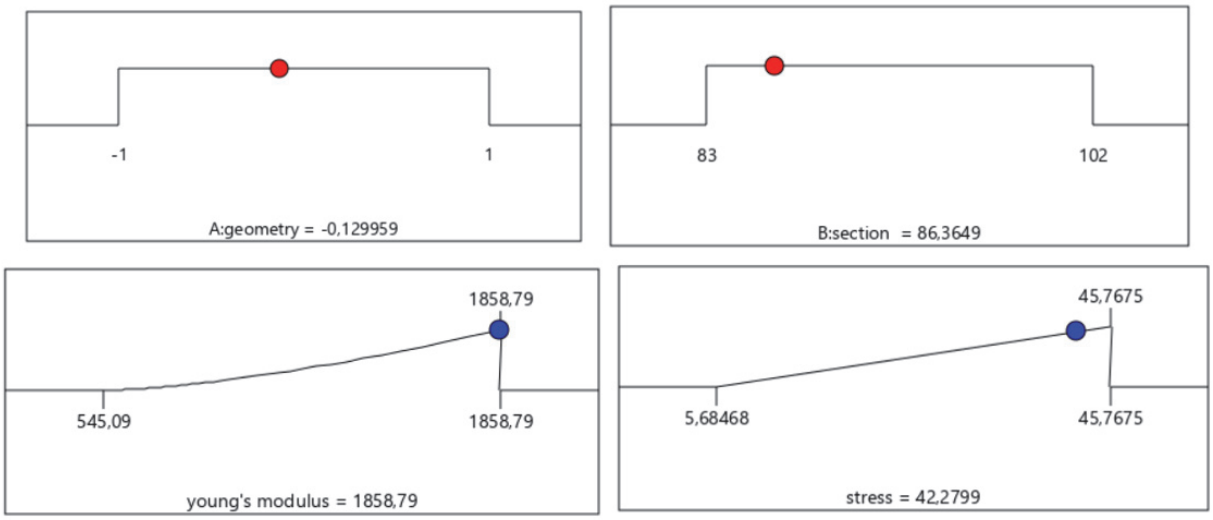

Figure 8: Numerical ramps for the optimal stress and Young‘s Modulus (Desirability = 0.956; Solution 1 out of 7).

ANN modelling

The ANN artificial neural network was selected to study the mechanical properties of Young‘s Modulus and to predict tensile test stresses. This is illustrated in Fig. 9, where we can see that it is a neural network composed of two input units, which represent the geometry of the samples and the sections of the samples, two hidden layers and an output layer (for the stress and the Young‘s Modulus). This network was formed using test data, in accordance with the analysis of statistics

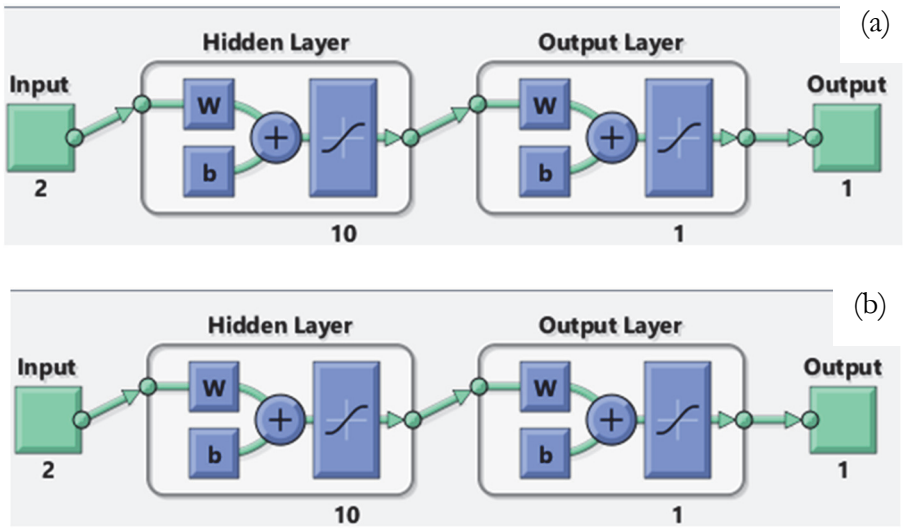

Figure 9: ANN Structure for :(a) Young‘s Modulus,(b) stress.

It was found that the correlation coefficients R^2 for the Young‘s Modulus and the stress were 0.984 and 0.981, respectively, according to Fig. 10-a. Fig. 10-b demonstrates the high precision of the artificial neural network ANN, as the experimental and expected results closely align with the 45° line. This confirms that the ANN model's predicted values for the training, validation, and test datasets were excellent. The mean squared error (MSE) was used to evaluate the model's accuracy. As illustrated in Fig. 11-A and Fig. 11-C, the randomly distributed data in Tab. 4 were split into 70%, 15%, and 15% for the training, validation, and testing datasets, respectively. As the accuracy of the ANN model improves, the MSE values approach 0. The MSE values are close to 100 for training, testing and validation for the Young module, while the MSE values are close to 10-2 for training, Tests and validation for stress. In the latter, the training, health and test lines on the same line have been merged into Fig. 11-b and Fig. 11-d, where we notice that the error is small thanks to the approach of training, testing and validation lines to the zero error line.

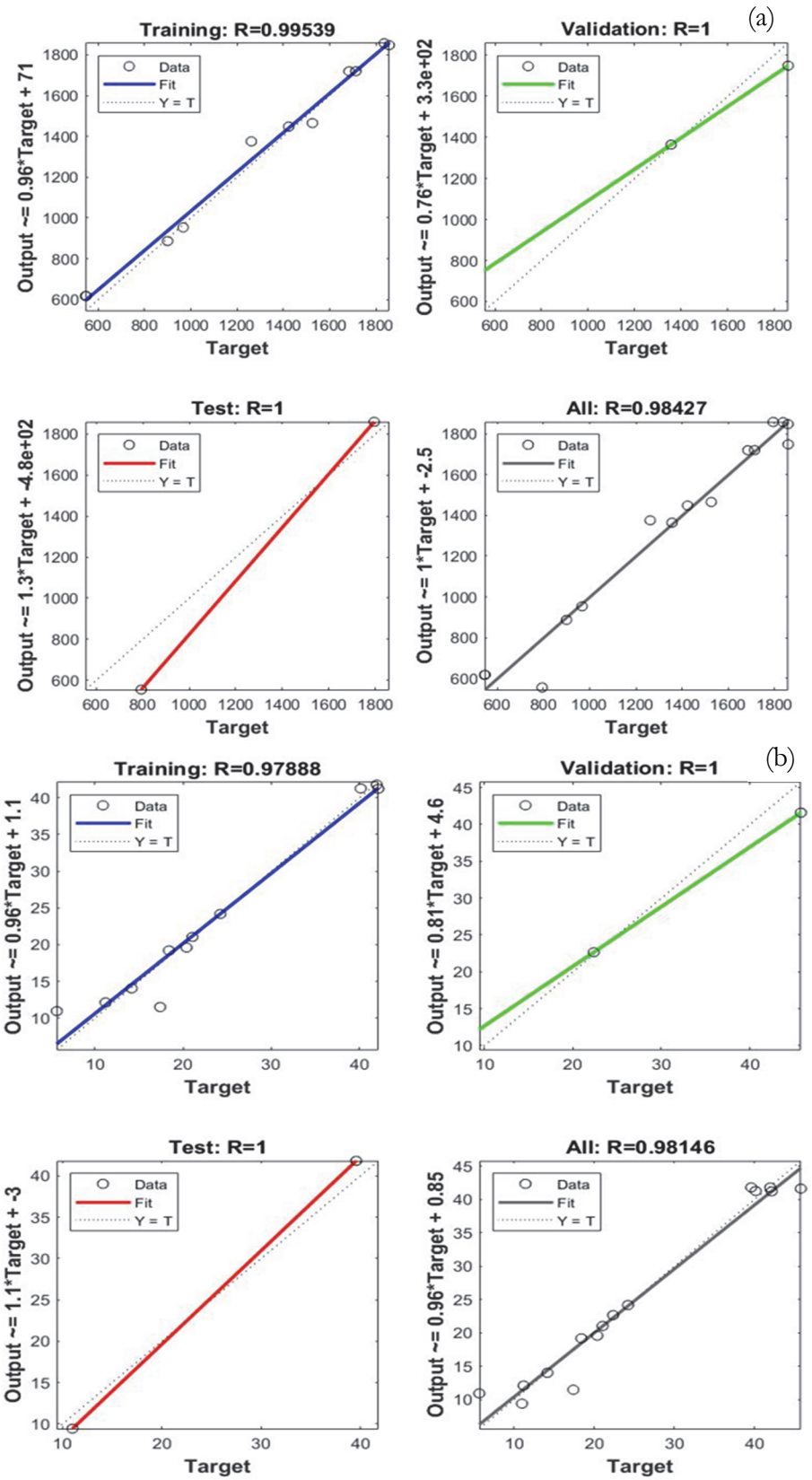

Figure 10: Predicted values versus experimental values of ANN models for training, validation, testing and all data:(a) Young's Modulus, (b) stress.

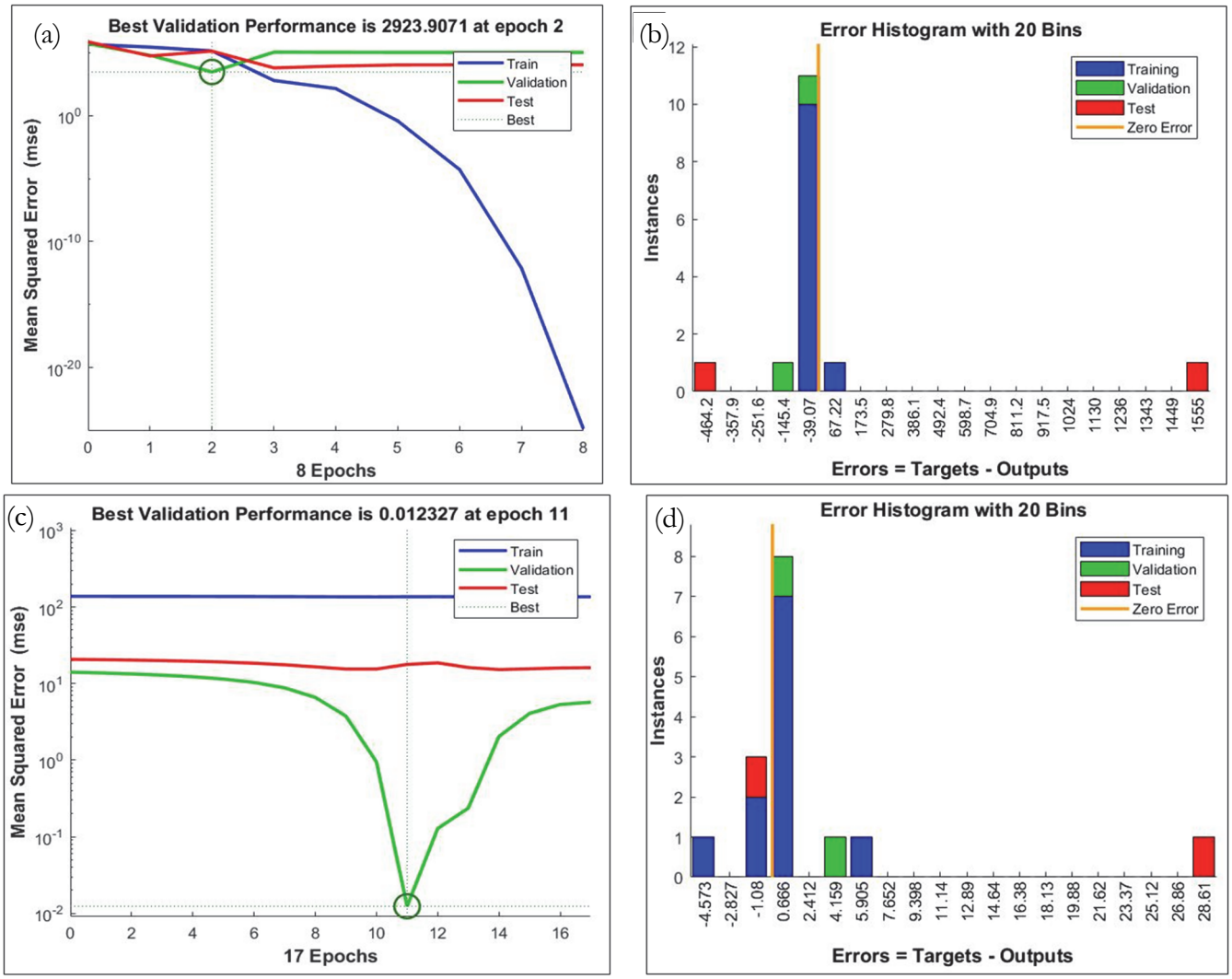

Figure 11: Mean square error and error histogram variation with respect to time for (a-b) Young's Modulus, (c-d) stress.

		samples	R
Young's Modulus	training	11	0.9812
	validation	2	0.9999
	testing	2	1
Maximum stress	training	11	0.9734
	validation	2	1
	testing	2	0.9999

Table 4: Allocation both of Young's Modulus and maximum stress used in ANN modeling.

Comparison between experimental, ANN and RSM models

Fig. 12 shows a comparison of the results between the ANN model and the RSM model with the experimental results for Young's Modulus and stress (Fig. 12-a and Fig. 12-b respectively). The results show that both models replicate the experimental results well, but that the ANN model provides a more accurate prediction than the RSM model. We can thus affirm that the prediction process of the ANN model is very accurate, with an overall coefficient of determination of 98% for Young's Modulus and stress respectively.

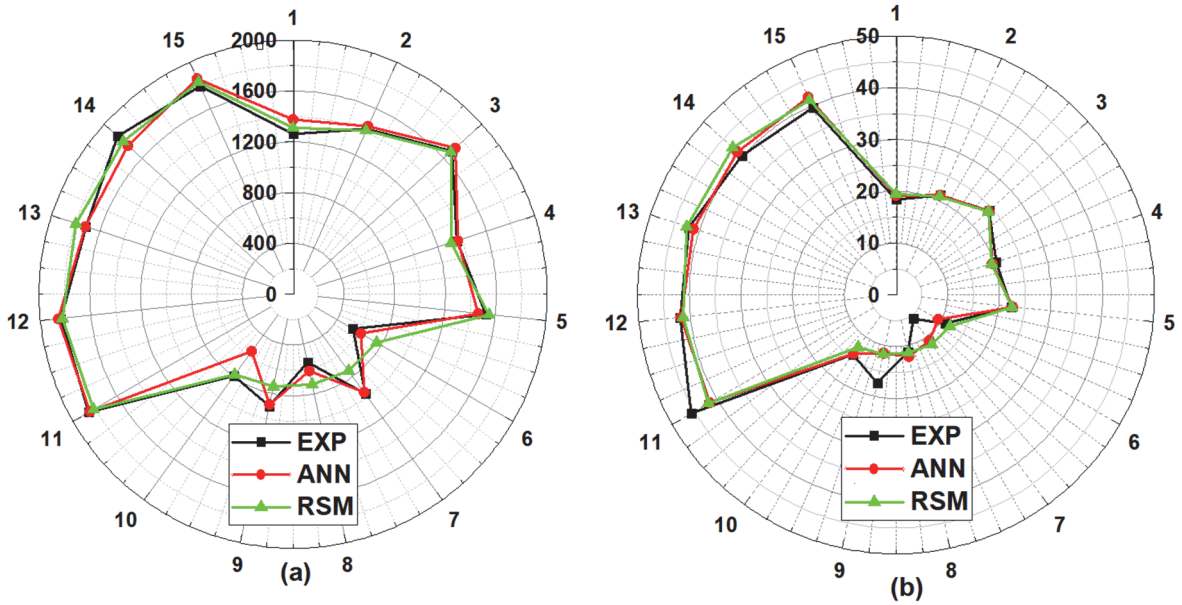

Figure 12: Comparison between experimental and predicted RSM and ANN models tensile data for: (a) Stress - (b) Young‘s Modulus.

CONCLUSION

For this research, a study was conducted on the mechanical properties of epoxy tensile samples (intact specimens, specimens with hole-notched and specimens with elliptical -notched) to evaluate the effect of sample geometry and cross-section on tensile test results. In addition, ANN and RSM models were used to predict mechanical properties, and the following results were obtained:

- The experimental results showed, through tensile tests of the samples studied, that the diameter and shape of the hole affect the mechanical properties of the materials. The lowest stress and Young‘s Modulus were observed in the specimen with elliptical -notched.
- The results we obtained with the ANN and RSM models were excellent, however, the ANN model can be considered the best since it can predict the coefficient and the Young stress due to its high correction coefficient, which is close to 1. As a result, the results of the ANN model are closer to the experimental results. As it is shown in the Tab.5

	ANN	RSM
correlation coefficients (R) of stress	0.98146	0.9598
correlation coefficients (R) of Young's Modulus	0.98427	0.9458

Table 5: Comparison between RSM and ANN models.

- We have obtained the results of the correlation coefficients (R) for ANN are excellent because correlation coefficients (R) of Young‘s Modulus were all greater than 0.984, with R = 0.99 for training, R = 1 for validation, R = 1 for test and R=0.984 for all .In terms of stress, the R's of all datasets were greater than 0.981 and R=0.97,1 and 1 for training, validation and test respectively .
- After comparing the experimental data to the expected data, the ANN modeling demonstrated an outstanding correlation, with an estimated average error value of 10^{-2} for stress and 10^{-0} for Young‘s Modulus.
- For the prediction of mechanical properties like stress and Young's Modulus values, an optimal network was employed with a training set size of 70%, validation set size of 15%, and test set size of 15%. The mean squared error (MSE) and the correlation coefficients were utilized as the evaluation metric in this study for determining the optimal network performance of ANN.

REFERENCE

[1] Chu, F., Qiu, S., Zhang, S., Xu, Z., Zhou Y., Luo, X., Jiang, X., Song, L., Hu, W. and Hu, Y. (2022). Exploration on structural Y. rules of highly efficient flame retardant unsaturated polyester resins. Journal of Colloid and Interface Science, 608, pp. 142-157. DOI, 10.1016/j.jcis.2021.09.124.

[2] Seraji, S.M., Song, P., Varley, R.J., Bourbigot, S., Voice,D.and Wang ,H. (2022). Fire-retardant unsaturated polyester thermosets, The state-of-the-art, challenges and opportunities. Chemical Engineering Journal, 430, p. 132785. DOI: 10.1016/j.cej.2021.132785.

[3] Mehta, L.B., Wadgaonkar, K.K. and Jagtap, R.N. (2019). Synthesis and characterization of high bio-based content unsaturated polyester resin for wood coating from itaconic acid, Effect of various reactive diluents as an alternative to styrene. Journal of Dispersion Science and Technology, 40(5), pp. 756-765. DOI: 10.1080/01932691.2018.1480964.

[4] Wei, L., Chen, X., Hong, K., Yuan, Z., Wang, L., Wang, H., Qiao, Z., Wang, X., Li, Z. and Wang, Z. (2019) Enhancement in mechanical properties of epoxy nanocomposites by Styrene-ethylene-butadiene-styrene grafted graphene oxide. Composite Interfaces, 26(2), pp. 141-156. DOI: 10.1080/09276440.2018.1481303.

[5] Rossi Canuto de Menezes, B., da Graça Sampaio, A., Morais da Silva, D., Larissa do Amaral Montanheiro, T. , Yumi Koga-Ito, C. and Patrocínio Thim, G. (2021). AgVO3 nanorods silanized with γ-MPS, An alternative for effective dispersion of AgVO3 in dental acrylic resins improving the mechanical properties. Applied Surface Science, 543, p. 148830. DOI: 10.1016/j.apsusc.2020.148830.

[6] Perea-Lowery, L., Gibreel, M., Vallittu, P.K. and L.V. Lassila, L.V. (2021). 3D-Printed vs. Heat-Polymerizing and Autopolymerizing Denture Base Acrylic Resins. Materials, 14(19), p. 5781.

[7] Qi, Y., Weng, Z., Kou, Y., Song, L., Li, J., Wang, J., Zhang, S., Liu, C. and Jian, X. (2021).Synthesize and introduce bio-based aromatic s-triazine in epoxy resin, Enabling extremely high thermal stability, mechanical properties, and flame retardancy to achieve high-performance sustainable polymers. Chemical Engineering Journal, 406, p. 126881. DOI: 10.1016/j.cej.2020.126881.

[8] Chen, H., Zhu, Z., Patil, D., Bajaj, D., Verghese, N., Jiang, Z. and Sue, H.-J. (2023). Mechanical properties of reactive polyetherimide-modified tetrafunctional epoxy systems. Polymer, 270, p. 125763. DOI: 10.1016/j.polymer.2023.125763.

[9] Dadrasi, A., Fooladpanjeh, S. and Alavi Gharahbagh, A. (2019). Interactions between HA/GO/epoxy resin nanocomposites, optimization, modeling and mechanical performance using central composite design and genetic algorithm. Journal of the Brazilian Society of Mechanical Sciences and Engineering, 41(2), p. 63. DOI: 10.1007/s40430-019-1564-7.

[10] Rai, A., Subramanian, N. and Chattopadhyay, A. (2017). Investigation of damage mechanisms in CNT nanocomposites using multiscale analysis. International Journal of Solids and Structures, 120, pp. 115-124. DOI: 10.1016/j.ijsolstr.2017.04.034.

[11] Chen, X., Liu, L., Pan, F., Mao, J., Xu, X. and Yan, T. (2015). Microstructure, electromagnetic shielding effectiveness and mechanical properties of Mg–Zn–Cu–Zr alloys. Materials Science and Engineering, B, 197, pp. 67-74. DOI: 10.1016/j.mseb.2015.03.012.

[12] Feng, Q., Yang, J., Yu, Y., Tian, F. , Zhang, B., Feng, M. and Wang, S. (2017).The ionic conductivity, mechanical performance and morphology of two-phase structural electrolytes based on polyethylene glycol, epoxy resin and nano-silica. Materials Science and Engineering, B, 219, pp. 37-44. DOI: 10.1016/j.mseb.2017.03.001.

[13] Ferdous, W., Manalo, A., Wong, H.S., Abousnina, R., AlAjarmeh, O.S., Zhuge, Y. and Schubel, P. (2020). Optimal design for epoxy polymer concrete based on mechanical properties and durability aspects. Construction and Building Materials, 232, p. 117229. DOI: 10.1016/j.conbuildmat.2019.117229.

[14] Cuan-Urquizo, E., Barocio, E., Tejada-Ortigoza, V., Pipes, R.B., Rodriguez, C.A. and Roman-Flores, A.(2019). Characterization of the Mechanical Properties of FFF Structures and Materials, A Review on the Experimental, Computational and Theoretical Approaches. Materials, 12(6), p. 895.

[15] Torrado, A.R. and Roberson, D.A. (2016). Failure Analysis and Anisotropy Evaluation of 3D-Printed Tensile Test Specimens of Different Geometries and Print Raster Patterns. Journal of Failure Analysis and Prevention, 16(1), pp. 154-164. DOI: 10.1007/s11668-016-0067-4.

[16] Öndürücü, A., Esendemir, Ü. and Tunay, R.F. (2012). Progressive failure analysis of glass–epoxy laminated composite pinned-joints. Materials & Design (1980-2015), 36, pp. 617-625. DOI: 10.1016/j.matdes.2011.11.031.

[17] Saada, K., Amroune, S., Zaoui, M., Houari, A., Madani, K. and Hachaichi, A. (2023). Experimental and Numerical Study of the Effect of the Presence of a Geometric Discontinuity of Variable Shape on the Tensile Strength of an Epoxy Polymer. Acta Mechanica et Automatica, 17(2), pp. 192-199.

[18] Habibi, M. and Laperrière, L. (2020).Digital image correlation and acoustic emission for damage analysis during tensile loading of open-hole flax laminates. Engineering Fracture Mechanics, 228, p. 106921. DOI: 10.1016/j.engfracmech.2020.106921.

[19] Han, D., Zhang, Y., Zhang, X.Y., Xie, Y.M. and Ren, X.(2023). Lightweight auxetic tubular metamaterials, Design and mechanical characteristics. Composite Structures, 311, p. 116849. DOI: 10.1016/j.compstruct.2023.116849.

[20] Deshwal, S., Kumar, A. and Chhabra, D. (2020.) Exercising hybrid statistical tools GA-RSM, GA-ANN and GA-ANFIS to optimize FDM process parameters for tensile strength improvement. CIRP Journal of Manufacturing Science and Technology, 31, pp. 189-199. DOI: 10.1016/j.cirpj.2020.05.009.

[21] Boumaaza, M., Belaadi, A., Bourchak, M., Juhany, K.A., Jawaid, M., Marvila, M.T. and de Azevedo, A.R.G. (2023). Optimization of flexural properties and thermal conductivity of Washingtonia plant biomass waste biochar reinforced bio-mortar. Journal of Materials Research and Technology, 23, pp. 3515-3536. DOI: 10.1016/j.jmrt.2023.02.009.

[22] Xi, X., Yin, Z., Yang, S. and Li, C.-Q. (2021). Using artificial neural network to predict the fracture properties of the interfacial transition zone of concrete at the meso-scale. Engineering Fracture Mechanics, 242, p. 107488. DOI: 10.1016/j.engfracmech.2020.107488.

[23] Mohammed, B.S., Achara, B.E., Liew, M.S., Alaloul, W.S. and Khed, V.C.(2019). Effects of elevated temperature on the tensile properties of NS-modified self-consolidating engineered cementitious composites and property optimization using response surface methodology (RSM). Construction and Building Materials, 206, pp. 449-469. DOI: 10.1016/j.conbuildmat.2019.02.033.

[24] Zamim, S.K., Faraj, N.S., Aidan, I.A., Al-Zwainy, F.M., AbdulQader, M.A. and Mohammed, I.A. (2019). Prediction of dust storms in construction projects using intelligent artificial neural network technology. Periodicals of Engineering and Natural Sciences, 7(4), pp. 1659-1666.

[25] Geyikçi, F., Kılıç, E., Çoruh, S. and Elevli, S. (2012). Modelling of lead adsorption from industrial sludge leachate on red mud by using RSM and ANN. Chemical Engineering Journal, 183, pp. 53-59. DOI: 10.1016/j.cej.2011.12.019.

[26] Boumaaza, M., Belaadi, A., Bourchak, M., Jawaid, M. and Hamid, S. (2022). Comparative study of flexural properties prediction of Washingtonia filifera rachis biochar bio-mortar by ANN and RSM models. Construction and Building Materials, 318, p. 125985. DOI: 10.1016/j.conbuildmat.2021.125985.

[27] Choudhary, P.K., Nanda, B.P. and Satapathy, A.(2022). Development, characterization, and parametric analysis of dry sliding wear behavior of epoxy-short betel nut fiber composite using response surface method and neural computation. Polymers and Polymer Composites, 30, p. 09673911211066722.

[28] Alhijazi, M., Safaei, B., Zeeshan, Q., Asmael, M., Harb, M. and Qin, Z. (2022). An Experimental and Metamodeling Approach to Tensile Properties of Natural Fibers Composites. Journal of Polymers and the Environment, 30(10), pp. 4377-4393. DOI: 10.1007/s10924-022-02514-1.

[29] Doblies, A., Boll, B. and Fiedler, B. (2019). Prediction of Thermal Exposure and Mechanical Behavior of Epoxy Resin Using Artificial Neural Networks and Fourier Transform Infrared Spectroscopy. Polymers, 11(2), p. 363.

[30] Kari, D.E., Benmounah, A., Bezazi, A., Bezzazi, B. and Baali, B.(2022). Evaluation of circumferential properties of Jute/Epoxy tubes manufactured by filament winding based on the fiber orientation.

[31] Goutham, E.R.S., Vamshi, Y., Namratha, M., Gupta, K.B., Chandrasekar, M. and Naveen, J.(2022). Influence of glass fibre hybridization on the open hole tensile properties of pineapple leaf fiber/epoxy composites. in AIP Conference Proceedings. AIP Publishing LLC.

[32] Zhu, l., Xu, F. and Shen, w. (2022). Numerical analyses of axial tension mechanisms of 3D orthogonal woven E-glass/epoxy composites with drilled holes. Textile Research Journal, 92(19-20), pp. 3478-3487.

[33] Yang, B., Fu, K., Lee, J. and Li, Y. (2021). Artificial Neural Network (ANN)-Based Residual Strength Prediction of Carbon Fibre Reinforced Composites (CFRCs) After Impact. Applied Composite Materials, 28(3), pp. 809-833. DOI: 10.1007/s10443-021-09891-1.

[34] Nwobi-Okoye, C.C. and Uzochukwu, C.U. (2020). RSM and ANN modeling for production of Al 6351/ egg shell reinforced composite, Multi objective optimization using genetic algorithm. Materials Today Communications, 22, p. 100674. DOI: 10.1016/j.mtcomm.2019.100674.

[35] Atuanya, C.U., Government, M.R., Nwobi-Okoye, C.C. and Onukwuli, O.D.(2014). Predicting the mechanical properties of date palm wood fibre-recycled low density polyethylene composite using artificial neural network. International Journal of Mechanical and Materials Engineering, 9(1), p. 7. DOI: 10.1186/s40712-014-0007-6.

[36] Pyl, L., K.-A. Kalteremidou, and Van Hemelrijck, D.(2019). Exploration of the design freedom of 3D printed continuous fibre-reinforced polymers in open-hole tensile strength tests. Composites Science and Technology, 171, pp. 135-151. DOI: 10.1016/j.compscitech.2018.12.021.

[37] Nanda, B.P. and Satapathy, A. (2021). An Analysis of the Sliding Wear Characteristics of Epoxy-Based Hybrid Composites Using Response Surface Method and Neural Computation. Journal of Natural Fibers, 18(12), pp. 2077-2091. DOI: 10.1080/15440478.2020.1722781.

[38] Omrani, E., P.L. Menezes, and Rohatgi, P.K. (2016). State of the art on tribological behavior of polymer matrix composites reinforced with natural fibers in the green materials world. Engineering Science and Technology, an International Journal, 19(2), pp. 717-736. DOI: 10.1016/j.jestch.2015.10.007.

[39] Teimouri, A., Barbaz Isfahani, R., Saber-Samandari, S. and Salehi, M.(2022). Experimental and numerical investigation on the effect of core-shell microcapsule sizes on mechanical properties of microcapsule-based polymers. Journal of Composite Materials, 56(18), pp. 2879-2894. DOI: 10.1177/00219983221107831.

[40] Zhang, K., C. Wang, Zhao, Y. and Bi, J. (2023). Experimental study on cracking behavior of concrete containing hole defects. Journal of Building Engineering, 65, p. 105806. DOI: 10.1016/j.jobe.2022.105806.

[41] Lin, Q., Cao, P., Meng, J., Cao, R. and Zhao, Z.(2020). Strength and failure characteristics of jointed rock mass with double circular holes under uniaxial compression, Insights from discrete element method modelling. Theoretical and Applied Fracture Mechanics, 109, p. 102692. DOI: 10.1016/j.tafmec.2020.102692.

[42] Azadi, M., H. Sayar, A. Ghasemi-Ghalebahman, and S.M. Jafari, Tensile loading rate effect on mechanical properties and failure mechanisms in open-hole carbon fiber reinforced polymer composites by acoustic emission approach. Composites Part B, Engineering, 2019. 158, pp. 448-458. DOI: 10.1016/j.compositesb.2018.09.103.

[43] Vahdati, M., Moradi, M. and Shamsborhan, M.(2020). Modeling and Optimization of the Yield Strength and Tensile Strength of Al7075 Butt Joint Produced by FSW and SFSW Using RSM and Desirability Function Method. Transactions of the Indian Institute of Metals, 73(10), pp. 2587-2600. DOI: 10.1007/s12666-020-02075-8.

[44] Heidarzadeh, A., Khodaverdizadeh, H., Mahmoudi, A. and Nazari, E. (2012).Tensile behavior of friction stir welded AA 6061-T4 aluminum alloy joints. Materials & Design, 37, pp. 166-173. DOI: 10.1016/j.matdes.2011.12.022.

[45] Bala, N., Napiah, M. and Kamaruddin, I. (2017). Performance evaluation of composite asphalt mixture modified with polyethylene and nanosilica. International Journal of Civil Engineering and Technology, 8(9), pp. 616-628.